SUPPLEMENTARY INFORMATION

In Pursuit of Next Generation N-heterocyclic Carbene-Stabilized Copper and Silver Precursors for Metalorganic Chemical Vapor Deposition and Atomic Layer Deposition Processes

Ilamparithy Selvakumar [1†], **Nils Boysen** [2†], **Marco Burger** [1], **Anjana Devi** [1,2*]

[1] Inorganic Materials Chemistry, Ruhr University Bochum, 44801 Bochum, Germany: E-mail: anjana.devi@ruhr-uni-bochum.de

[2] Fraunhofer IMS, 47057 Duisburg, Germany

* Correspondence: anjana.devi@ruhr-uni-bochum.de

† The authors contributed equally to this work

Abstract:

Volatile, reactive, and thermally stable organometallic copper and silver complexes are of significant interest as precursors for the metalorganic chemical vapor deposition (MOCVD) and atomic layer deposition (ALD) of ultra-thin metallic films. Well-established Cu^{I} and Ag^{I} precursors are commonly stabilized by halogens, phosphorous, silicon, and oxygen, potentially leading to the incorporation of these elements as impurities in the thin films. These precursors are typically stabilized by a neutral and anionic ligand. Recent advancements were established by the stabilization of these complexes using N-heterocyclic carbenes (NHCs) as neutral ligands. To further enhance the reactivity, in this study the anionic ligand is sequentially changed from β-diketonates to β-ketoiminates and β-diketiminates, yielding two new Cu^{I} and two new Ag^{I} NHC-stabilized complexes in the general form of [M(NHC)(R)] (M = Cu, Ag; R = β-ketoiminate, β-diketiminate). The synthesized complexes were comparatively analyzed in solid, dissolved, and gaseous states. Furthermore, the thermal properties were investigated to assess their potential application in MOCVD or ALD. Among the newly synthesized complexes, the β-diketiminate-based [Cu(*t*BuNHC)(NacNacMe)] was identified to be the most suitable candidate as a precursor for Cu thin film deposition. The resulting halogen-, oxygen-, and silicon-free Cu^{I} and Ag^{I} precursors for MOCVD and ALD applications are established for the first time and set a new baseline for coinage metal precursors.

Supporting Figures

1. **NMR spectrometry data**

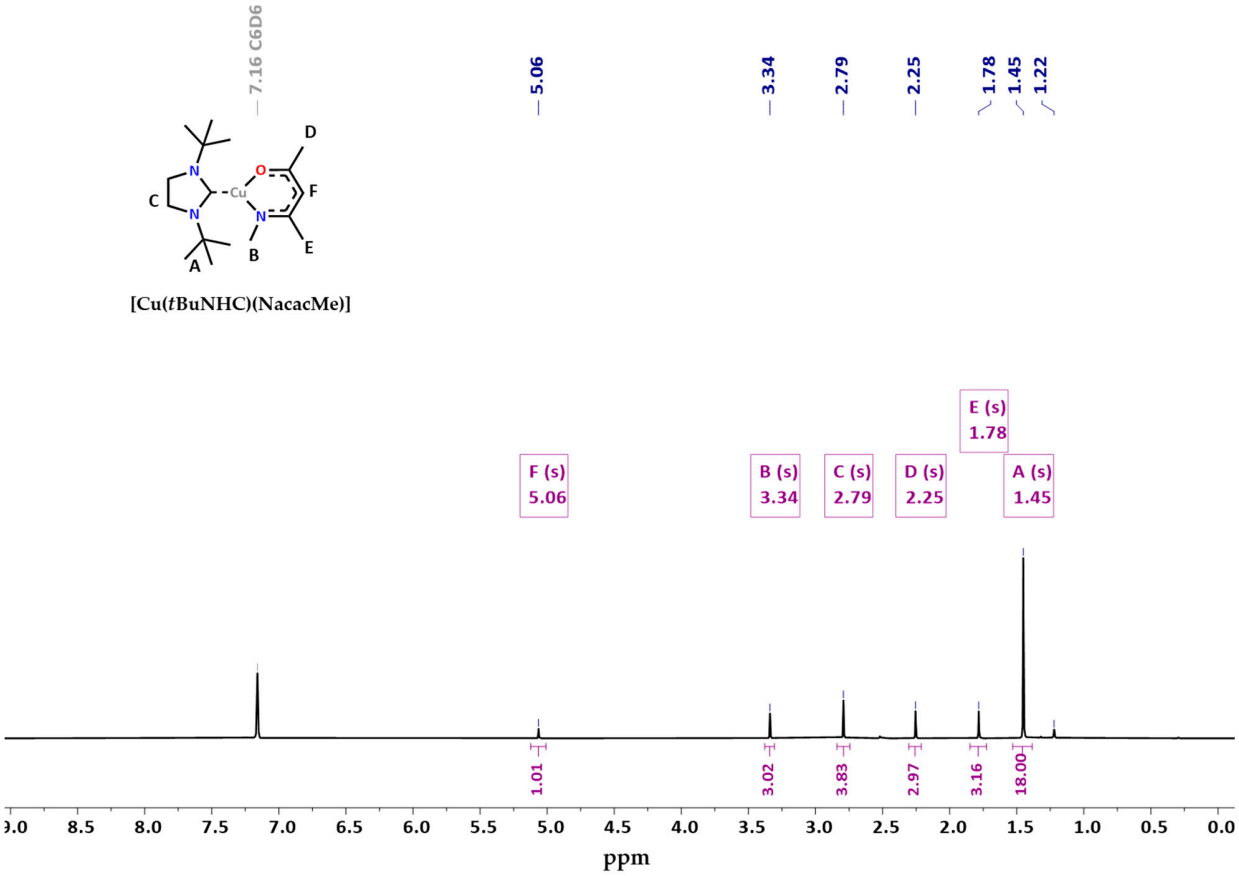

Figure S1. ^{1}H-NMR spectrum of [Cu(*t*BuNHC)(NacacMe)] in C_6D_6 solvent. The integrals are referenced to the singlet A at 1.45 ppm.

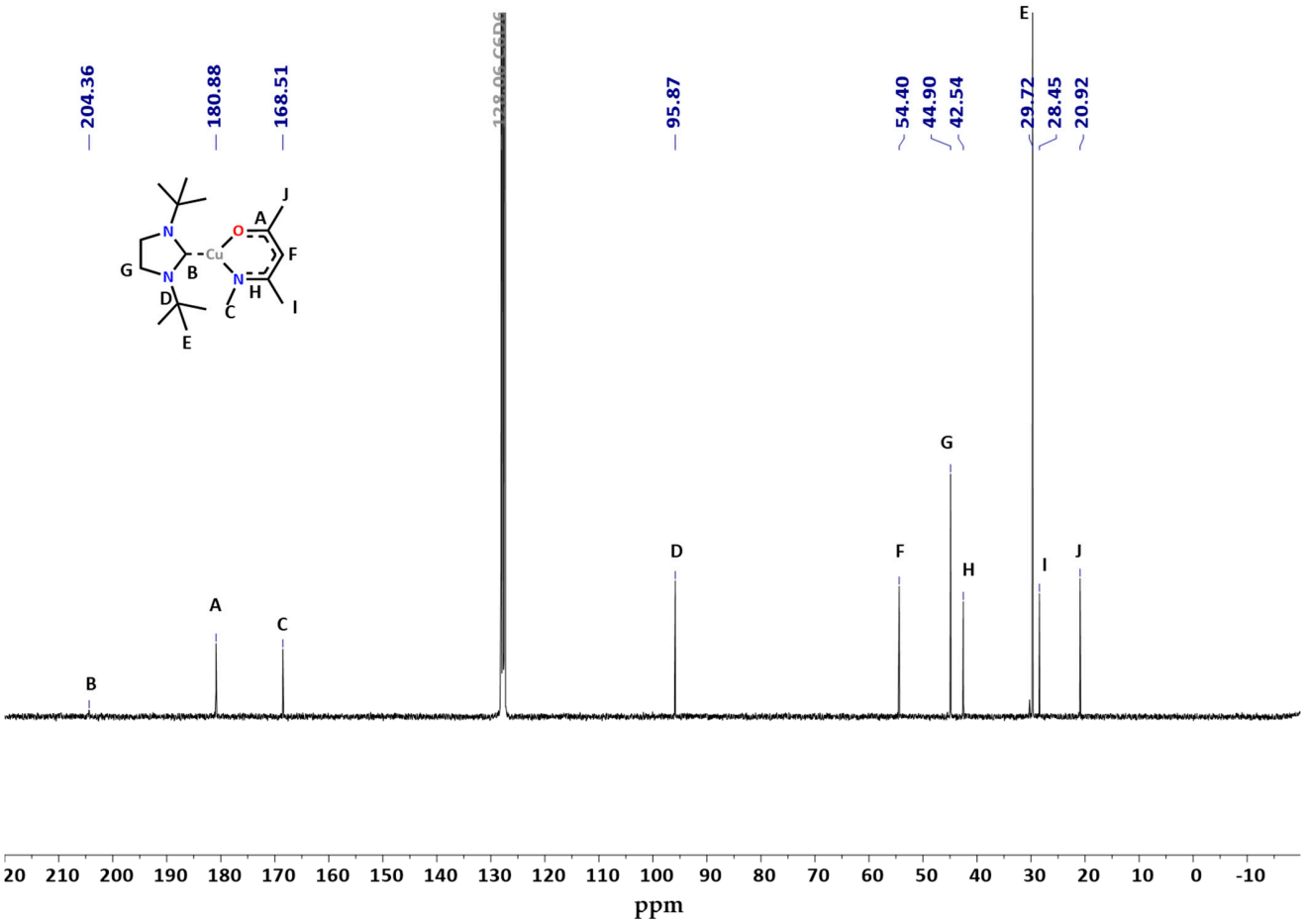

Figure S2. ^{13}C-NMR spectrum of [Cu(*t*BuNHC)(NacacMe)] in C_6D_6 solvent. The characteristic carbene peak B and carbonyl carbon peak A is observed distinctively.

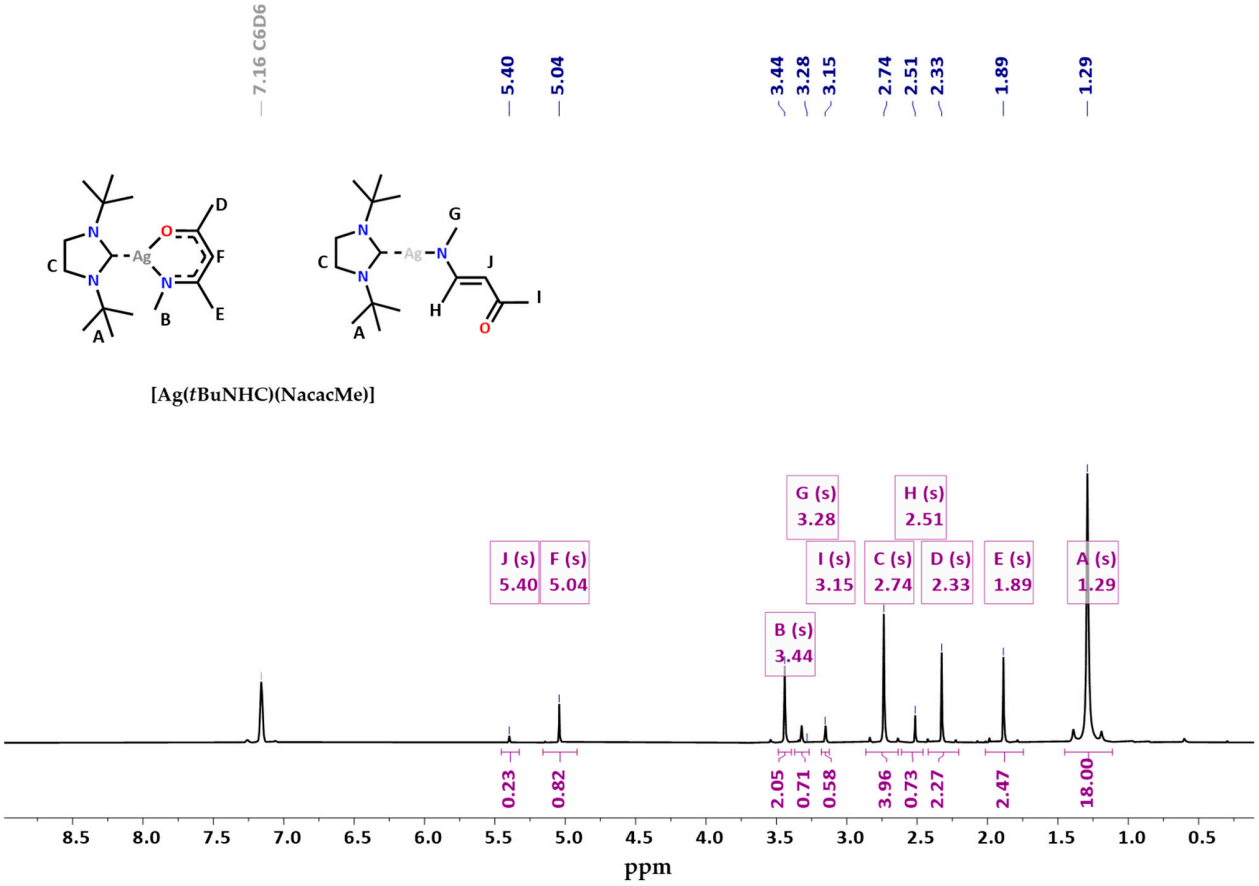

Figure S3. ^{1}H-NMR spectrum of [Ag(*t*BuNHC)(NacacMe)] in C_6D_6 solvent. The characteristic carbene peak B and carbonyl carbon peak A is observed distinctively.

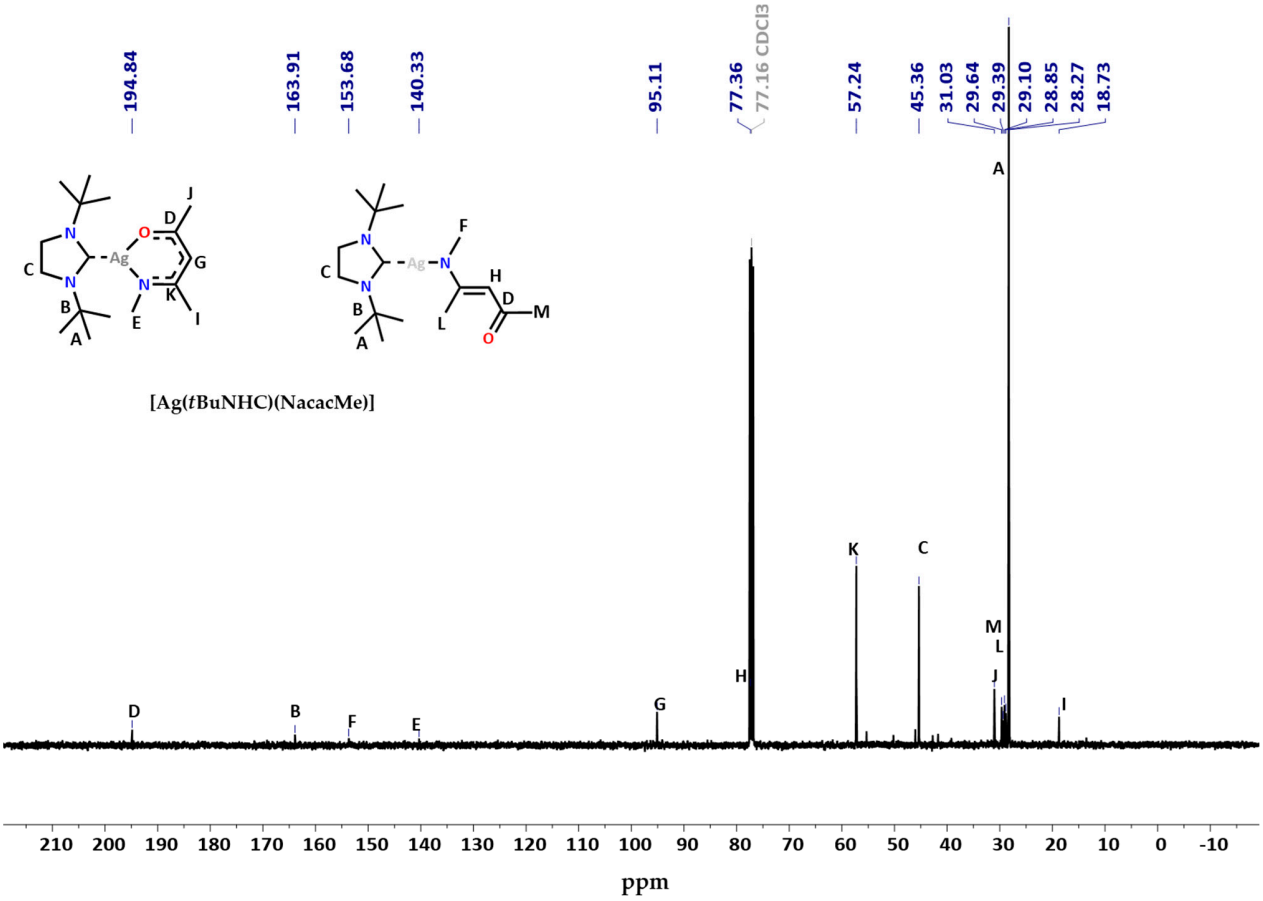

Figure S4. ^{13}C-NMR spectrum of [Ag(*t*BuNHC)(NacacMe)] in C_6D_6 solvent.

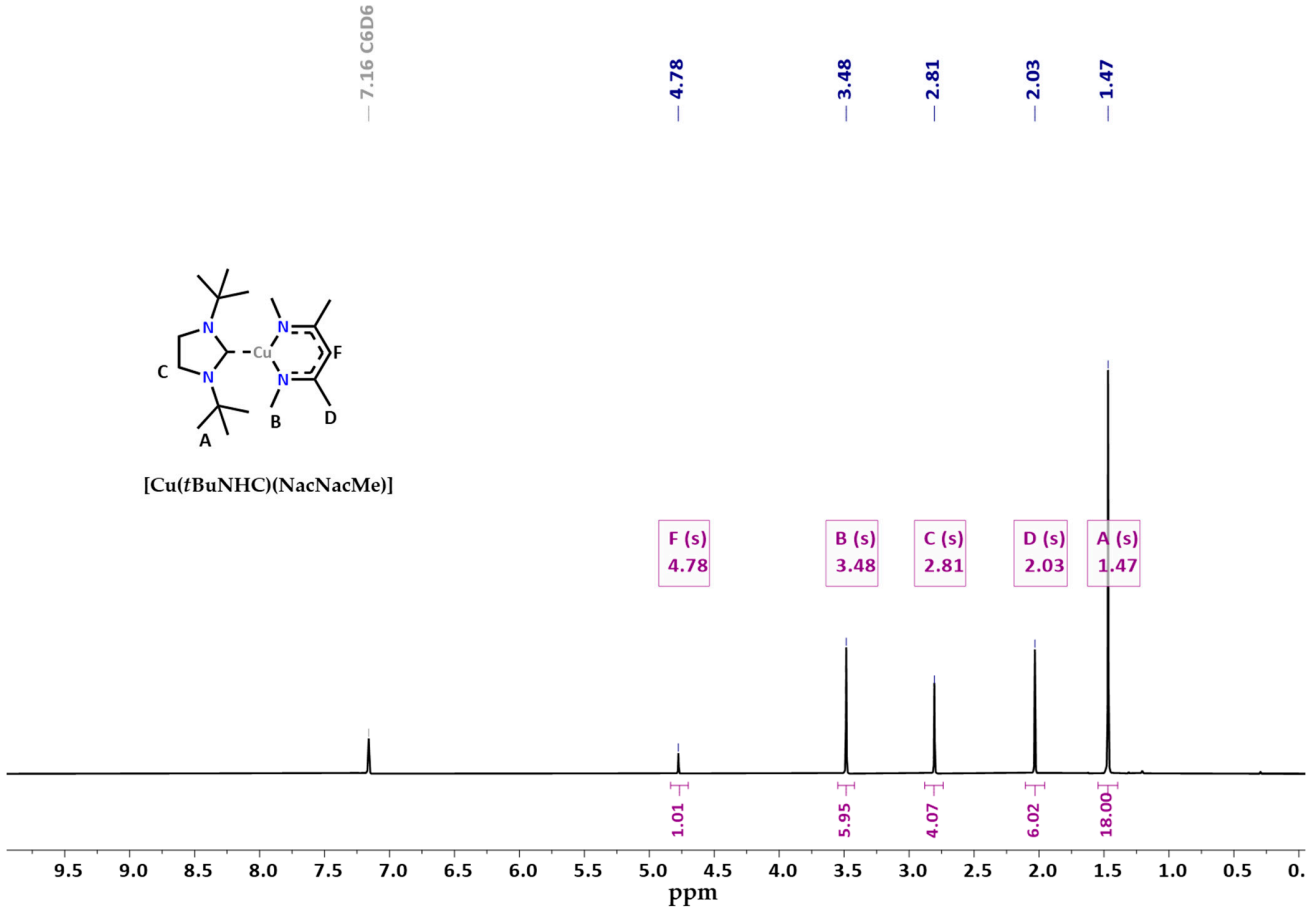

Figure S5. ^{1}H-NMR spectrum of [Cu(*t*BuNHC)(NacNacMe)] in C_6D_6 solvent.

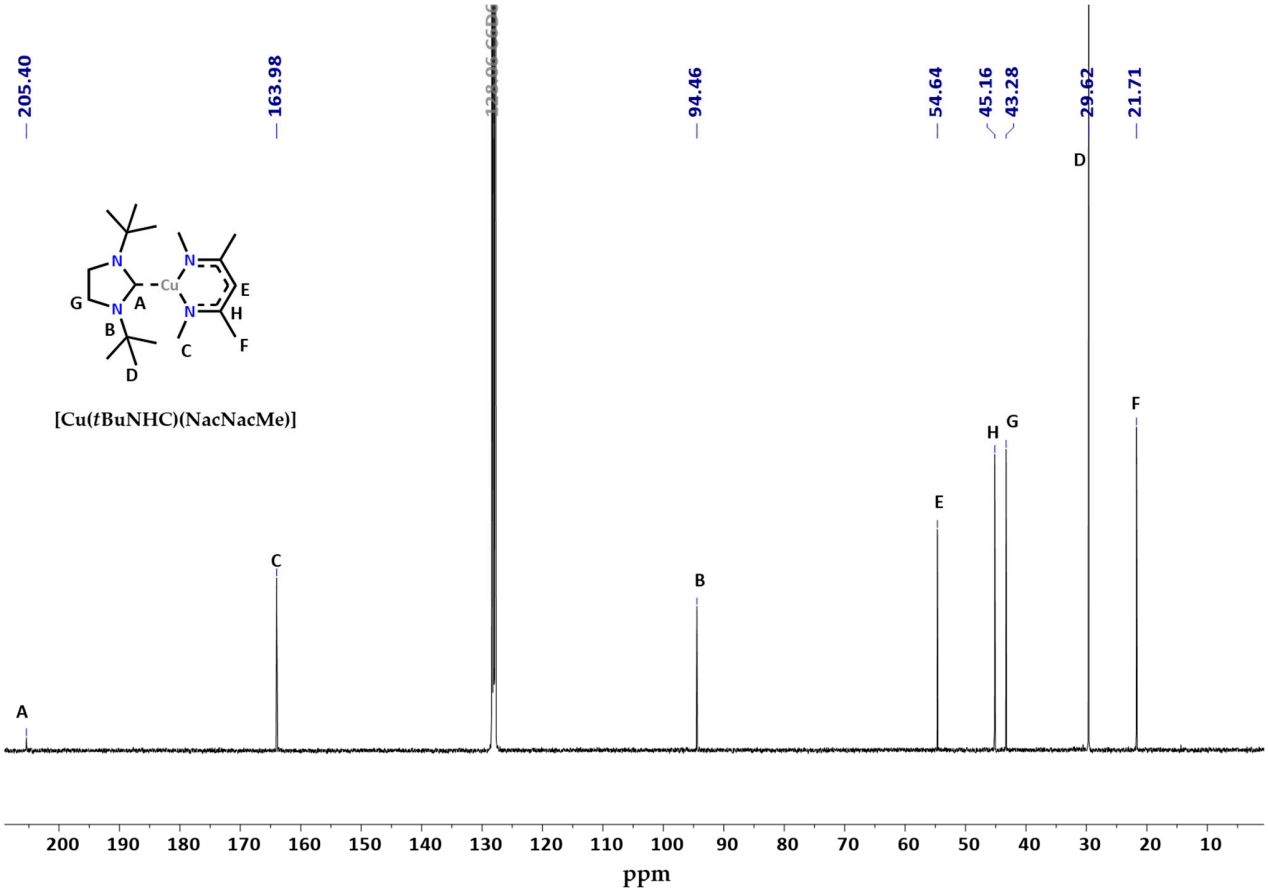

Figure S6. ^{13}C-NMR spectrum of [Cu(*t*BuNHC)(NacNacMe)] in C_6D_6 solvent. Peak A corresponds to carbene and peak B corresponds to $((CH_3)_3CN)$. Peak B and peak C can be differentiated due to the partial pi bond character on the NacNacMe amine, which increases the shielding relative to the t-butyl carbon.

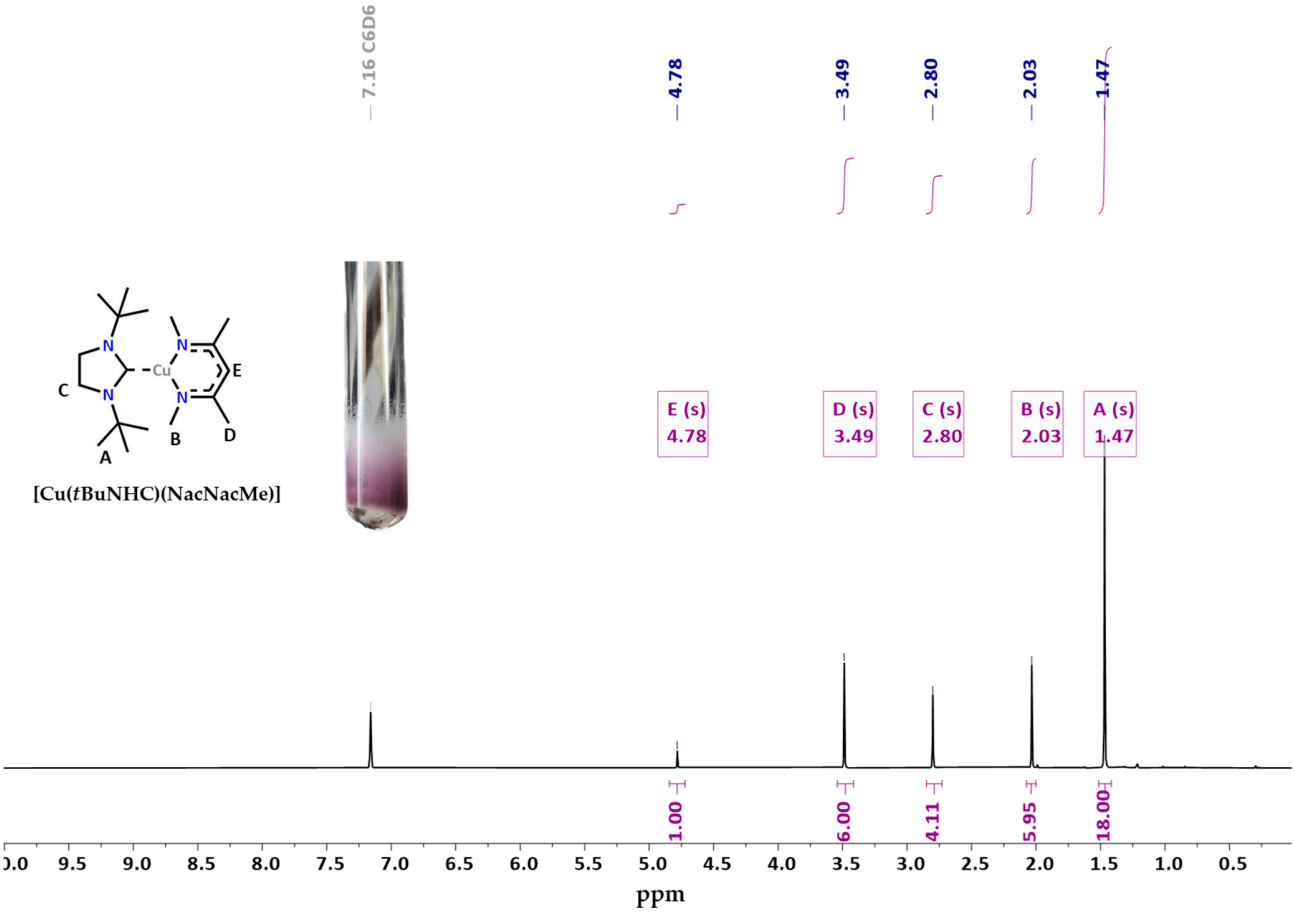

Figure S7. ^{1}H-NMR spectrum of [Cu(*t*BuNHC)(NacNacMe)] in C_6D_6 solvent, upon sublimation at 110 °C and 1 mbar pressure. The integrals are referenced to singlet A. The inset image shows the result of a fast sublimation in a small Schlenk flask, where no visible residue was found. In comparison to the figure S7, the spectra have no visible difference thus no sign of decomposition is found, upon sublimation.

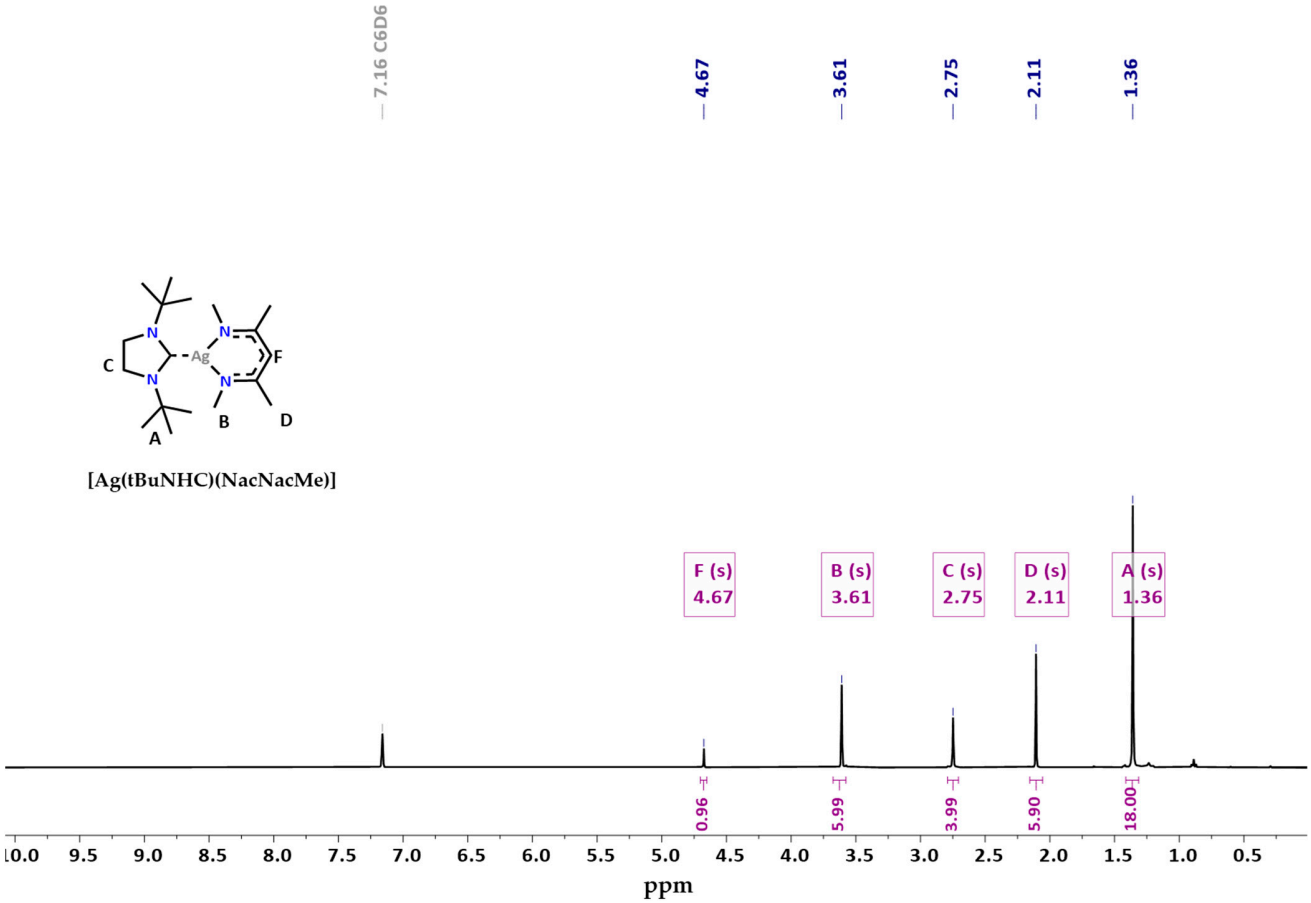

Figure S8. ^{1}H-NMR spectrum of [Ag(*t*BuNHC)(NacNacMe)] in C_6D_6 solvent. The integrals are referenced to peak A.

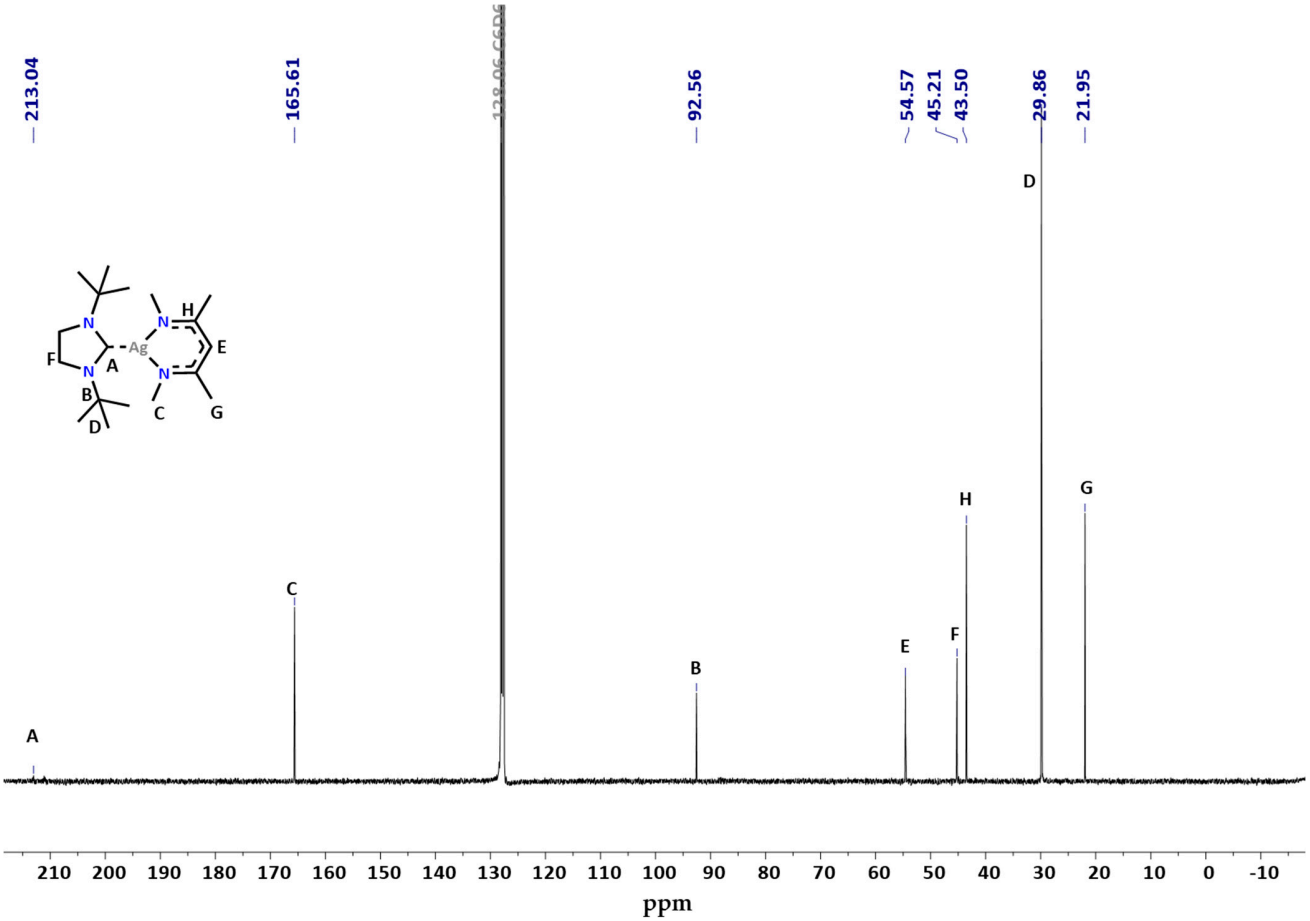

Figure S9. ^{13}C-NMR spectrum of [Ag(*t*BuNHC)(NacNacMe)] in C_6D_6 solvent.

Figure S10. [Ag(*t*BuNHC)(NacNacMe)] upon a quick sublimation using a heat gun (>200 °C). Majority of the complex seemed to have thermally decomposed to silver, which is visually seen as a silver mirror. Thus, a very good choice as a silver precursor for MOCVD.

2. Mass spectrometry data

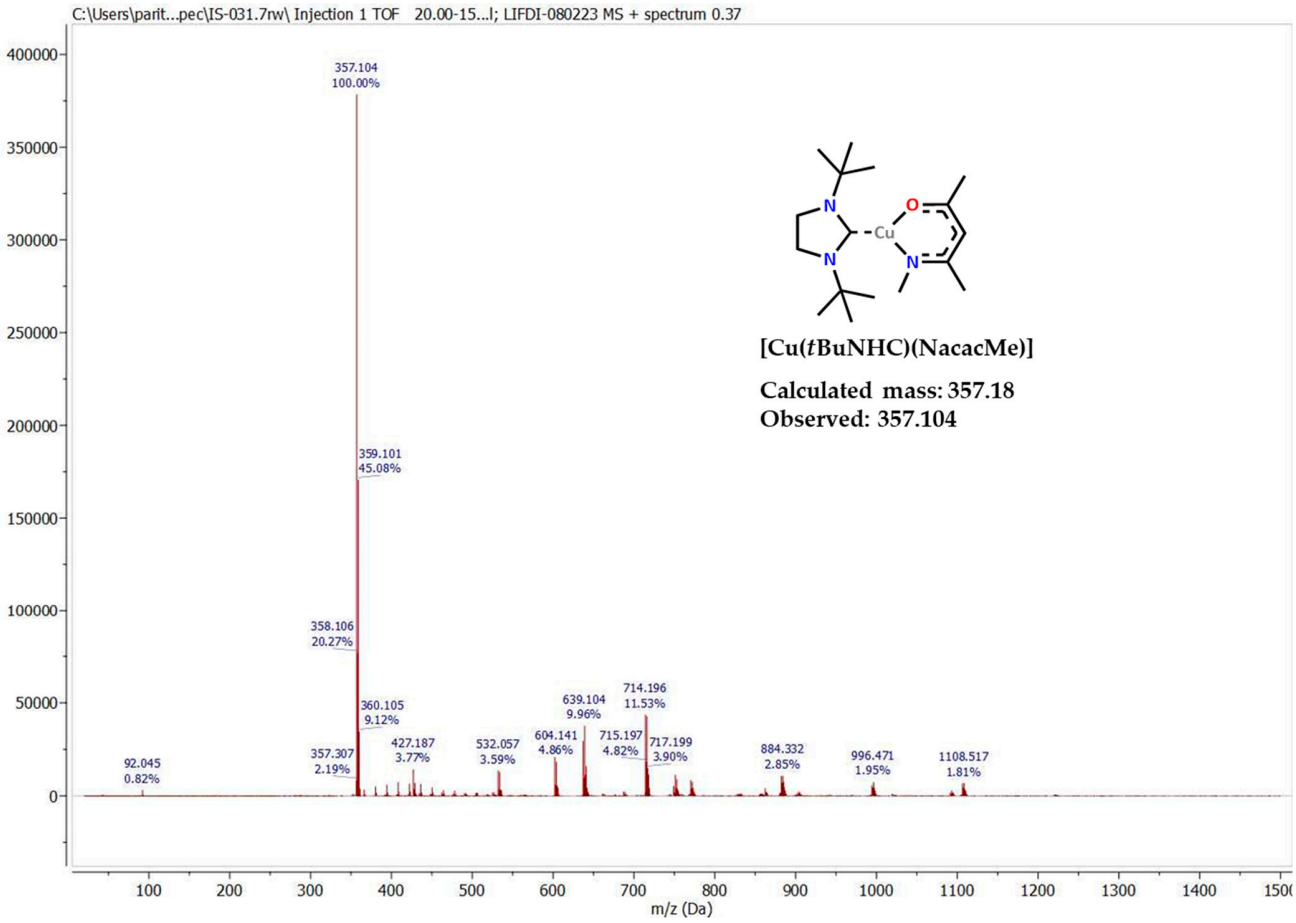

Figure S11. LIFDI-Mass spectra of [Cu(*t*BuNHC)(NacacMe)] in toluene as the solvent. The very soft ionization produced by LIFDI proved to be essential in determining the molecular ion peak as seen in the figure. A dimer at 714.196 m/z can be observed as well.

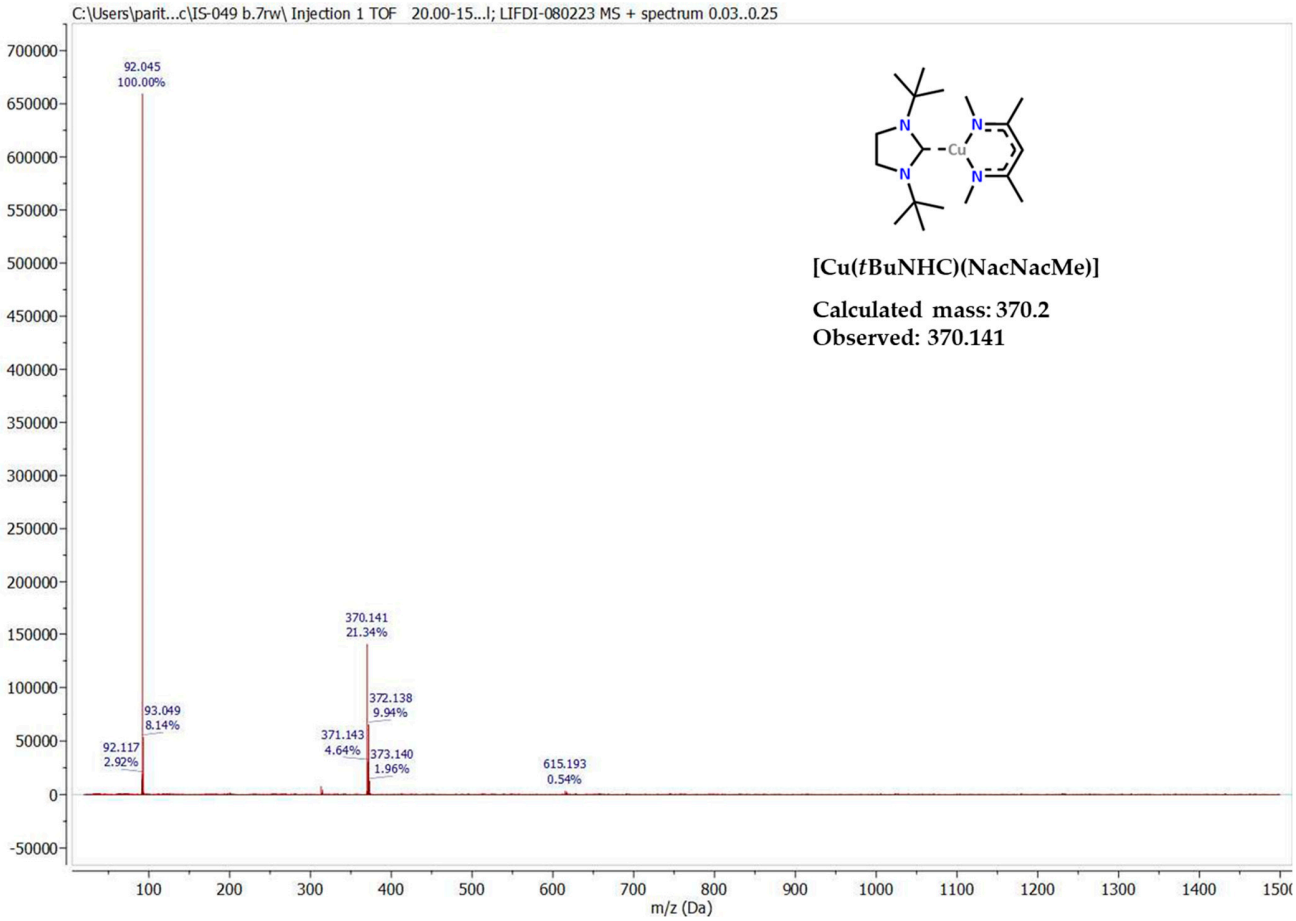

Figure S12. LIFDI-Mass spectra of [Cu(*t*BuNHC)(NacacMe)] in toluene as the solvent. The high abundance peak is from the major toluene fragment whereas, the molecular ion peak can be observed clearly at 370.141 m/z. Definitive fragment patterns could be assigned for the other minor peaks.

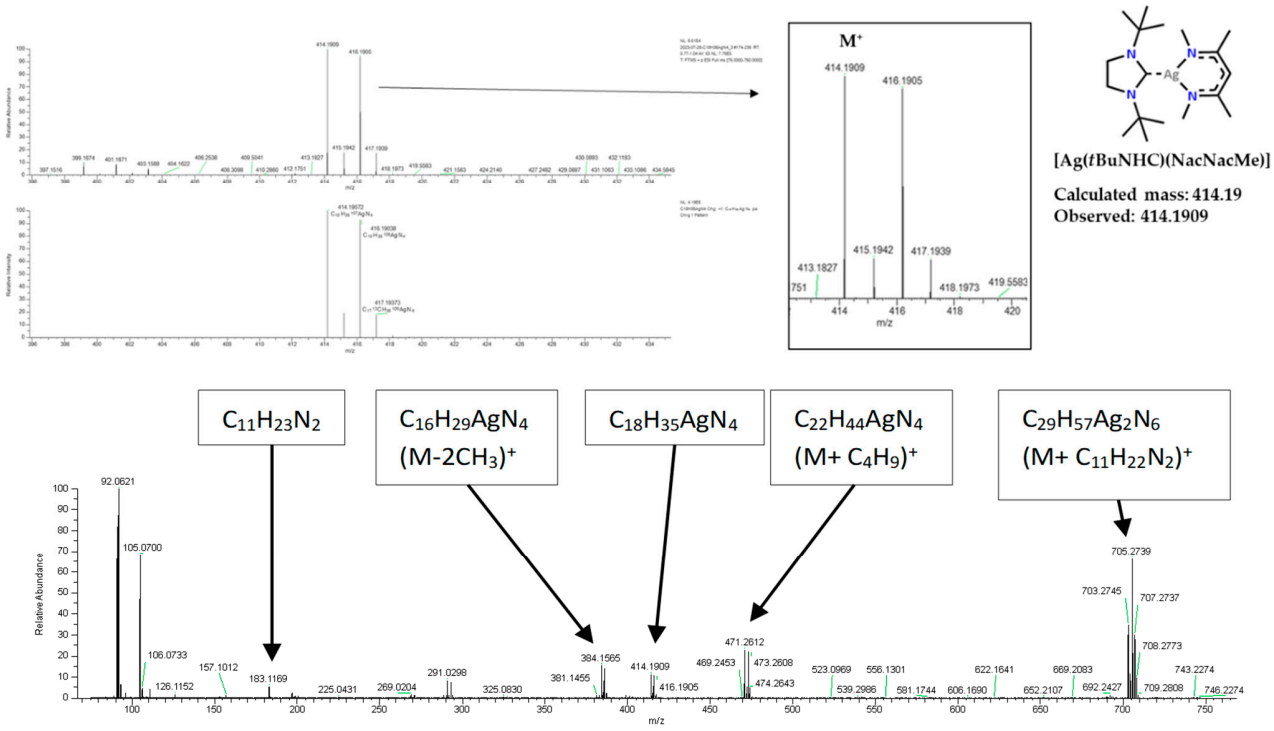

Figure S13. The [Ag(tBuNHC)(NacNacMe)] was subjected to high resolution LIFDI-MS (orbitrap) visibly producing a molecular ion peak at 414.1909 m/z. The unstable nature of this silver complex could also be observed with its various unexpected fragments, like the dual *t*BuNHC attached silver complex at 471.2612 m/z and a possible dimer complex at 705.2739 m/z. This immediate formation of products again highlights the photosensitivity of the Ag metal which could have been the result of the low ionization nature of LIFDI.

3. Vapour pressure plots

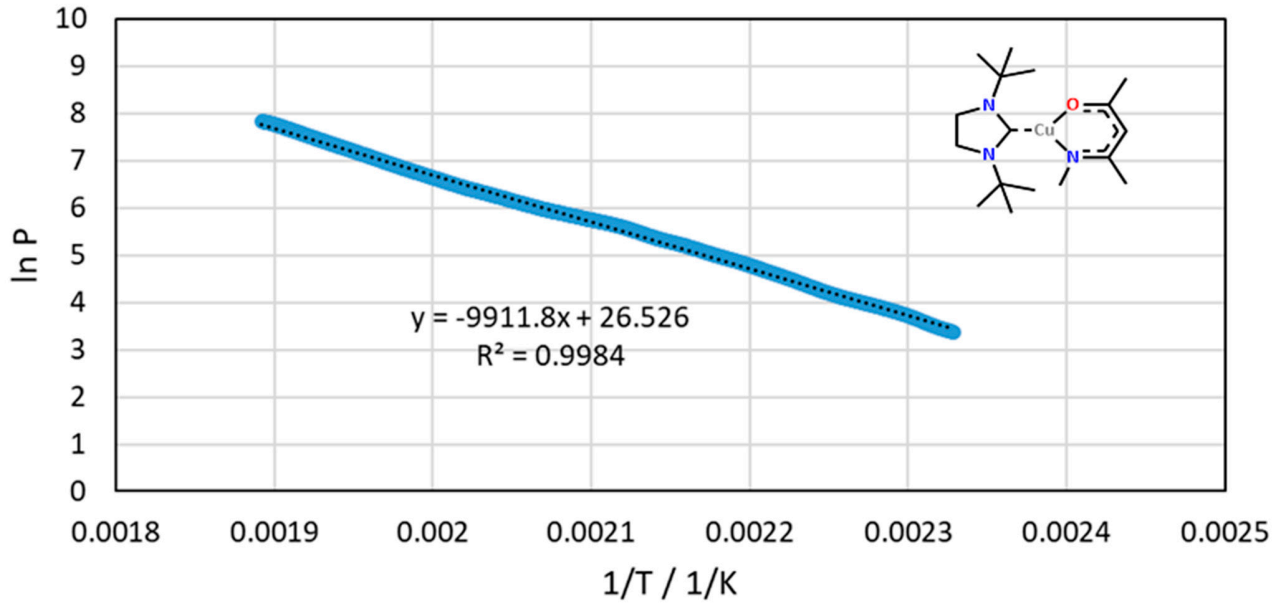

Figure S14. Vapour pressure graph calculated using the Clausius–Clapeyron equation from the differential thermogravimetry data (DTG).[1] The 1 Torr temperature was calculated to be 185.02 °C with an error factor of 0.3.

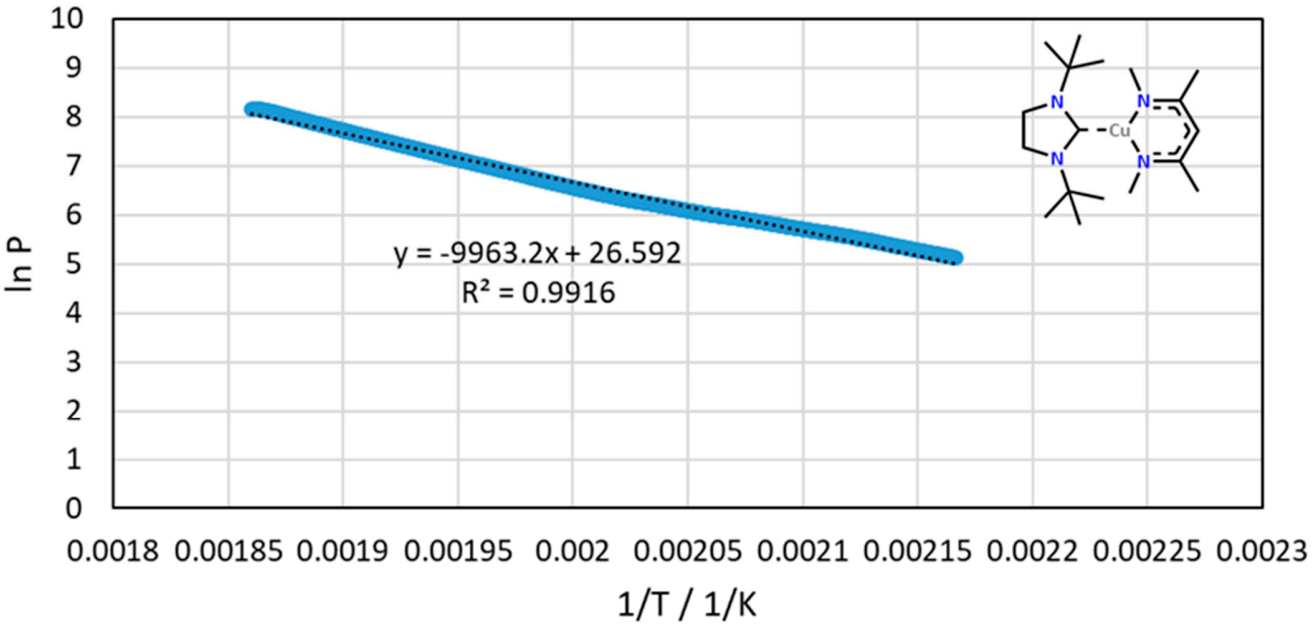

Figure S15. Vapour pressure graph calculated using the Clausius–Clapeyron equation from the differential thermogravimetry data (DTG). The 1 Torr temperature was calculated to be 186.00 °C with an error factor of 0.779. The decrease in vapor pressure upon increase in temperature is observed owing to its negative slope.[1]

4. XRD patterns of the residue from TG measurements

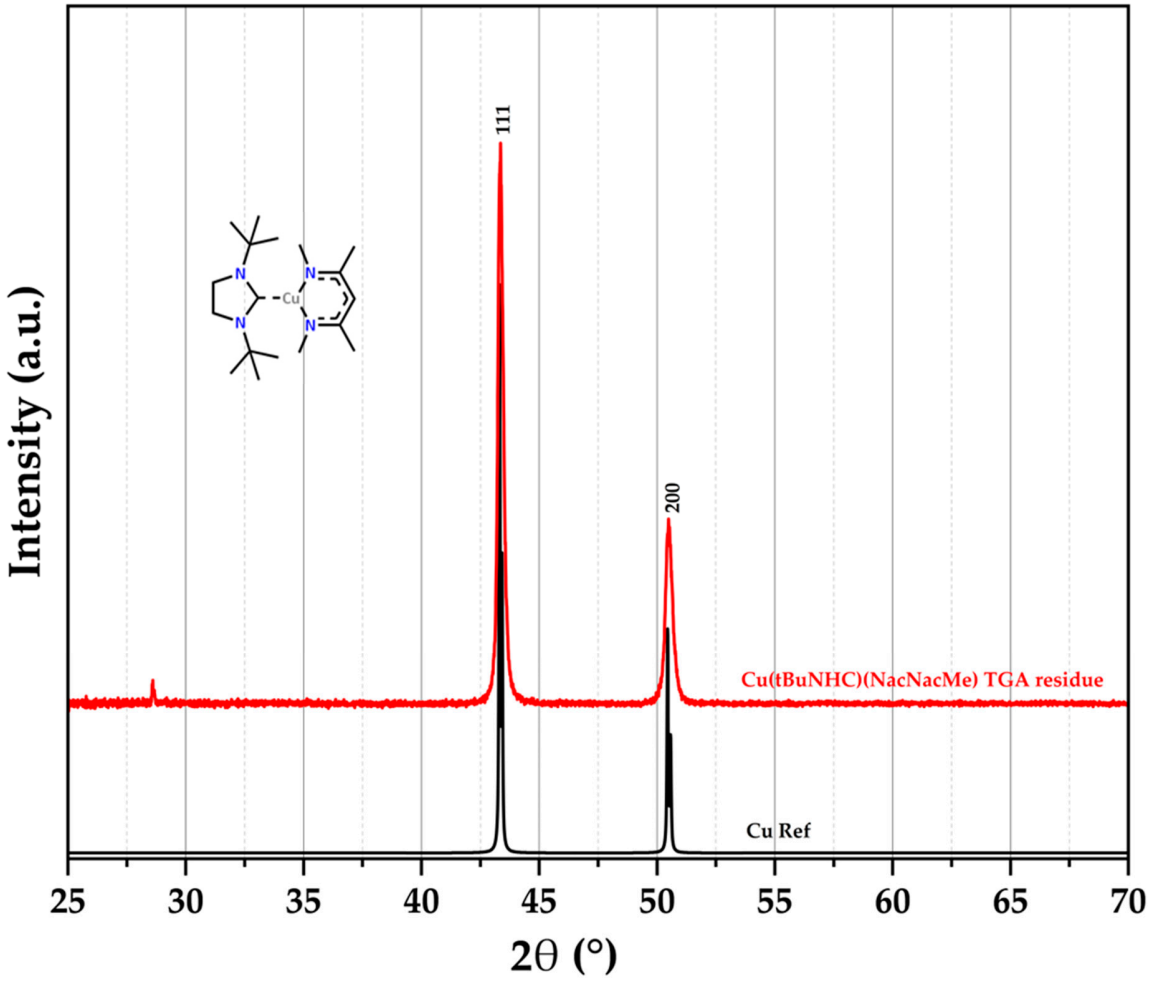

Figure S16. Powder XRD of the residue of [Cu(*t*BuNHC)(NacNacMe)] from TG analysis. (inset) The crystalline pattern of metallic copper (COD: 4105681) matches with the XRD of the residue, thus confirming the 16% rest mass to be the metallic copper.[2]

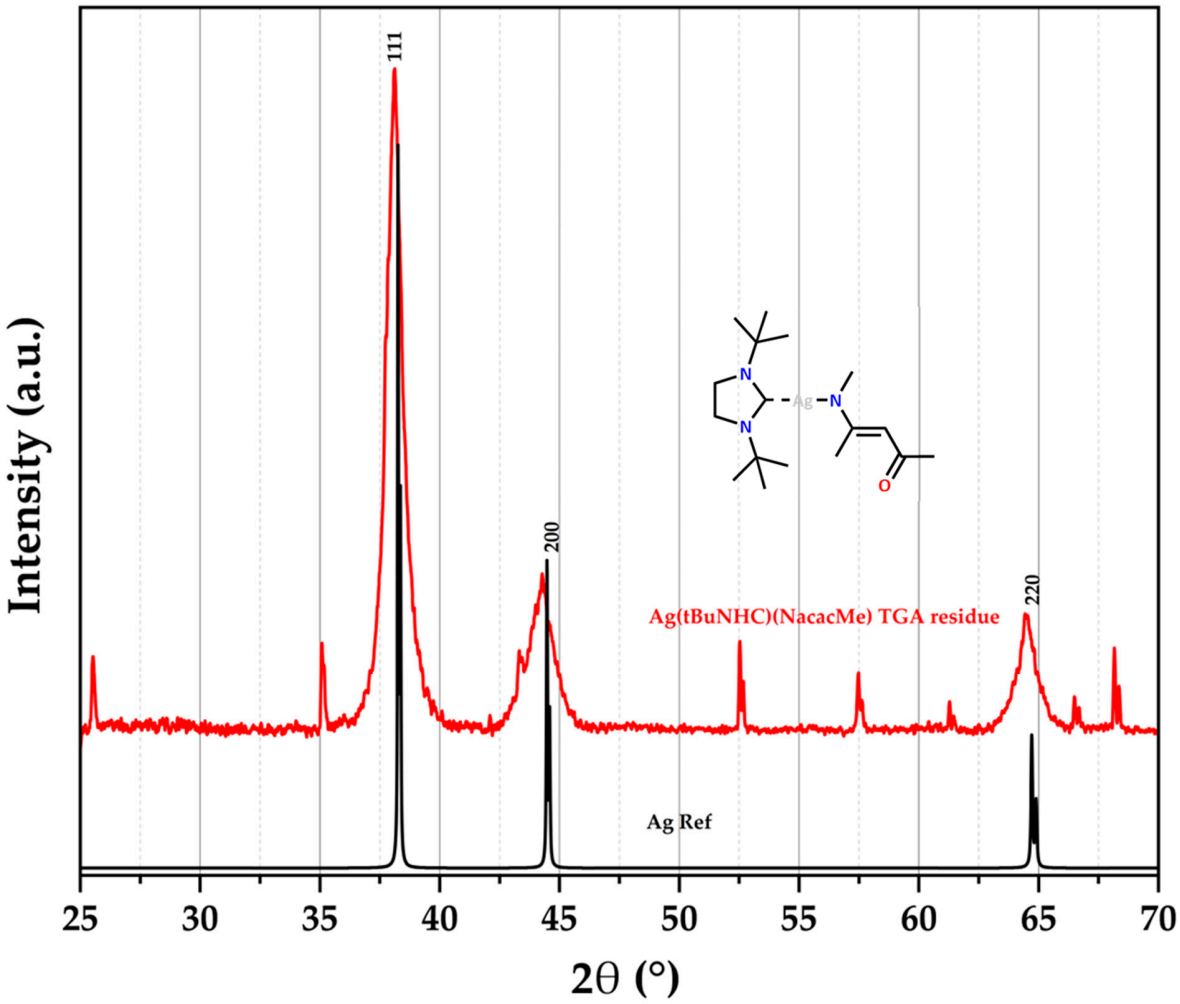

Figure S17. Powder XRD of the residue of [Ag(*t*BuNHC)(NacacMe)] from TG analysis. (inset) The residual XRD pattern reveals reflections matching the crystalline Ag XRD pattern (COD: 1509146). Additional reflections are also observed, possibly arising from the no fully decomposed precursor. [3]

Table S1. Prominent Cu^{I} and Ag^{I} precursors employed in ALD and MOCVD.

Cu^{I}-Precursors	**1% Mass loss (°C)**	**Heteroatoms**	**Ref**
[Cu(TMVS)(hfac)}	50-60	Si, F, O	4
[Cu(*i*PrNHC)(HMDS)]	90-100	Si, N	5
[Cu(*t*BuNHC)(acac)]	115	N, O	6
Ag^{I}-Precursors	1% Mass loss (°C)	Heteroatoms	Ref
[Ag(PEt3)(fod)]	95-100	P, F, O	8
[Ag(*t*BuNHC)(HMDS)]	90-100	Si, N	7

5. References

1. Price, D. Vapor Pressure Determination by Thermogravimetry. *Thermochim. Acta* - THERMOCHIM ACTA 2001, 367, 253–262, doi:10.1016/S0040-6031(00)00676-6.
2. Smura, C.F.; Parker, D.R.; Zbiri, M.; Johnson, M.R.; Gál, Z.A.; Clarke, S.J. High-Spin Cobalt(II) Ions in Square Planar Coordination: Structures and Magnetism of the Oxysulfides $Sr_2CoO_2Cu_2S_2$ and $Ba_2CoO_2Cu_2S_2$ and Their Solid Solution. *J. Am. Chem. Soc.* 2011, 133, 2691–2705, doi:10.1021/ja109553u.
3. Owen, E.A.; Williams, G.I. A Low-Temperature X-Ray Camera. *J. Sci. Instrum*. 1954, 31, 49, doi:10.1088/0950-7671/31/2/305.
4. Moon, D.-Y.; Kim, W.-S.; Kim, T.-S.; Kang, B.-W.; Park, J.-W.; Yeom, S.J.; Kim, J.H. Atomic Layer Deposition of Copper Seed Layers from a (Hfac)Cu(VTMOS) Precursor. *JKPS* 2009, 54, 1330–1333, doi:10.3938/jkps.54.1330.
5. Coyle, J.P.; Dey, G.; Sirianni, E.R.; Kemell, M.L.; Yap, G.P.A.; Ritala, M.; Leskelä, M.; Elliott, S.D.; Barry, S.T. Deposition of Copper by Plasma-Enhanced Atomic Layer Deposition Using a Novel N-Heterocyclic Carbene Precursor. *Chem. Mater.* 2013, 25, 1132–1138, doi:10.1021/cm400215q.
6. Boysen, N.; Misimi, B.; Muriqi, A.; Wree, J.-L.; Hasselmann, T.; Rogalla, D.; Haeger, T.; Theirich, D.; Nolan, M.; Riedl, T.; et al. A Carbene Stabilized Precursor for the Spatial Atomic Layer Deposition of Copper Thin Films. *Chem. Commun.* 2020, 56, 13752–13755, doi:10.1039/D0CC05781A.
7. Boysen, N.; Hasselmann, T.; Karle, S.; Rogalla, D.; Theirich, D.; Winter, M.; Riedl, T.; Devi, A. An N-Heterocyclic Carbene Based Silver Precursor for Plasma-Enhanced Spatial Atomic Layer Deposition of Silver Thin Films at Atmospheric Pressure. *Angew. Chem.* 2018, 57, 16224–16227, doi:10.1002/anie.201808586.
8. Minjauw, M.M.; Solano, E.; Sree, S.P.; Asapu, R.; Van Daele, M.; Ramachandran, R.K.; Heremans, G.; Verbruggen, S.W.; Lenaerts, S.; Martens, J.A.; et al. Plasma-Enhanced Atomic Layer Deposition of Silver Using Ag(Fod)(PEt3) and NH3-Plasma. *Chem. Mater*. 2017, 29, 7114–7121, doi:10.1021/acs.chemmater.7b00690.